

---

---

# Facilities for Dark Energy Investigations

Convener: David Weinberg

Deborah Bard, Kyle Dawson, Olivier Doré, Joshua Frieman, Karl Gebhardt, Michael Levi, Jason Rhodes

## 1 Overview

The discovery of cosmic acceleration has inspired ambitious experimental and observational efforts to understand its origin. Many of these take the form of large astronomical surveys, sometimes using new, special-purpose instrumentation, and in some cases entirely new facilities. These efforts are frequently referred to as “dark energy experiments,” which is the terminology we will adopt in this Report; we will not try to draw any fine distinctions between “experiments” and “observations.” The basic thrust of these experiments is to measure the history of expansion and growth of structure in the universe with steadily increasing precision over the broadest achievable range of redshifts. The hope is that these measurements may eventually reveal discrepancies with the predictions of a simple cosmological constant model, perhaps pointing towards a particular class of dynamical field or a breakdown of General Relativity (GR) on cosmological scales. The approach is in many ways analogous to high-energy physics experiments that pursue increasing measurement precision or new ranges of energy, hoping to “break” the standard model in a way that points towards deeper physics that underpins it.

Most existing and planned dark energy experiments employ one or more of the following approaches:

1. Wide-field imaging, to measure weak gravitational lensing, the galaxy content and weak lensing signal of galaxy clusters, and angular clustering of galaxies in bins of photometrically estimated redshift.
2. Synoptic observations to discover and monitor Type Ia supernovae, using them to measure the distance-redshift relation.
3. Wide-field spectroscopy, to map the clustering of galaxies, quasars, and the Ly $\alpha$  forest and thereby measure distances and expansion rates with baryon acoustic oscillations (BAO) and the history of structure growth with redshift-space distortions (RSD).

These techniques are reviewed in detail by [1] and discussed in many of the Snowmass CF5 Reports. The same wide-field imaging facilities are often well adapted to both of the first two approaches, which can be interleaved in a coherent observing strategy. However, a supernova survey also requires spectroscopic observations to determine redshifts and confirm the Type Ia identification. These spectroscopic observations are usually carried out from telescopes other than the ones used for discovery and photometric monitoring, and the spectroscopic observations may require significantly more observing time (and larger aperture telescopes) than the discovery and monitoring themselves. To relieve the stringent demands of obtaining

“real-time” spectroscopy, there is increasing focus on the use of photometrically defined Type Ia samples with subsequent spectroscopy to obtain host-galaxy redshifts, though in these cases one still needs spectroscopic observations of a subset of SNe to estimate contamination rates.

Large cosmological surveys that have completed their observations, though not necessarily their final analyses, include the imaging and spectroscopic surveys of the Sloan Digital Sky Survey (SDSS-I and II, [2]), the SDSS-II supernova survey [3, 4], all conducted from the Sloan Foundation 2.5m telescope in New Mexico [5], and the Supernova Legacy Survey (SNLS, [6]) and CFHTLenS weak lensing survey [7], both conducted from the Canada-France-Hawaii 3.6m telescope.

In this Report we briefly summarize some of the major dark energy experiments that are currently in operation or are planned to start operations in the next decade. We restrict our discussion to projects that are U.S.-led or, in some cases, where U.S. scientists are playing a significant supporting role. Many of these projects are described in publicly available documents that run for tens or hundreds of pages. Here we have confined our discussion of each project to two pages, with selective references to additional documentation. These facilities and experiments are referred to in many of the other CF5 Reports. The projects that we summarize are:

- The Baryon Oscillation Spectroscopic Survey (BOSS), a wide-field spectroscopic survey on the Sloan 2.5m telescope, now entering its final year of observations.
- The Dark Energy Survey (DES), a wide-field imaging survey and supernova survey on the Blanco 4m telescope, using the recently commissioned Dark Energy Camera, commencing survey operations in Fall 2013 and continuing for five years.
- The extended Baryon Oscillation Spectroscopic Survey (eBOSS), a wide-field spectroscopic survey on the Sloan 2.5m telescope extending to higher redshifts than the BOSS galaxy survey. The intended start is summer 2014, extending for six years.
- The Subaru Hyper-Suprime Camera (HSC) and Prime Focus Spectrograph (PFS), wide-field imaging and spectroscopic instruments that will be used for cosmological surveys from the Subaru 8.4m telescope. Intended starts are 2014 (HSC) and 2018 for (PFS).
- The Hobby-Eberly Telescope Dark Energy Experiment (HETDEX), which will use wide-field spectroscopy on the HET to survey Ly $\alpha$  emitters at  $1.9 < z < 3.5$ . Intended start is fall 2014, with a 3-year duration and extension to 5 years if needed.
- The Dark Energy Spectroscopic Instrument (DESI), a wide-field spectroscopic instrument that will carry out dark energy surveys from the Mayall 4m telescope. Intended start is 2018, with 5-year survey duration.
- The Large Synoptic Survey Telescope (LSST), a new 8.4m telescope equipped with an enormous wide-field optical camera, dedicated to wide-field imaging and synoptic time-domain surveys. Intended start is 2020, with 10-year duration.
- Euclid, a 1.2m space telescope dedicated to a large area weak lensing survey with optical imaging and a large area spectroscopic survey with slitless infrared spectroscopy. Scheduled launch is 2020, with 6-year duration of the prime mission.
- The Wide-Field Infrared Survey Telescope (WFIRST), which in its most recently proposed design would use a 2.4m telescope for wide-field imaging and slitless spectroscopic surveys and a supernova survey, in addition to other astronomical surveys. Intended launch is early 2020s, with 6-year duration of the prime mission.

Before describing these facilities individually, it is worth making two general points. First, the data sets constructed for “dark energy experiments” are very rich, supporting a wide range of other scientific objectives. Some of these lie within the broader scope of Cosmic Frontiers — in particular, precision measurements of galaxy clustering and weak lensing are powerful probes of neutrino masses, unknown relativistic species, inflation physics, and perhaps the nature of dark matter. Others lie outside Cosmic Frontiers, such as galaxy and quasar evolution, the physics of the intergalactic medium, and the structure and history of the Milky Way and neighboring galaxies. This broad scientific reach is a primary reason that the astronomical community has committed resources, expertise, and effort to these experiments. LSST and WFIRST would certainly not have achieved their top billing in the Astro2010 Decadal Survey if not for their enormous, broad ranging impact across many fields of astronomy, including dark energy. Conversely, the broad astronomical community benefits from the resources, expertises, and effort that the high energy physics community has brought to these and other projects.

Second, there are important routes to testing dark energy and modified gravity models that lie outside the scope of the facilities described here. These include direct measurements of the Hubble constant, precision tests of gravity in the solar system or the laboratory, and studies of gravitational effects in different galactic and large scale environments (see the Novel Probes Report). The critical clue to the origin of cosmic acceleration could come from a surprising direction, including, perhaps, a theoretical breakthrough. However, “mainstream” dark energy experiments offer a clear path towards steadily improving precision of cosmic expansion and structure growth measurements, thus allowing ever more stringent tests of a wide class of theories of dark energy and modified gravity.

## 2 The Baryon Oscillation Spectroscopic Survey (BOSS)

BOSS is the largest of the four surveys that comprise SDSS-III (SDSS = Sloan Digital Sky Survey). Its defining goals are to measure the distance-redshift relation  $D_A(z)$  and expansion rate  $H(z)$  with percent-level precision through baryon acoustic oscillations (BAO), using luminous galaxies to probe redshifts  $z \approx 0.2-0.7$  and the Ly $\alpha$  forest to probe redshifts  $z \approx 2-3.5$ . BOSS builds on the Luminous Red Galaxy (LRG) survey [8] of SDSS-I and II [9], which enabled the first detection of BAO ([10], alongside a contemporaneous detection in the 2dF Galaxy Redshift Survey by [11]) and its refinement into a tool for precision cosmology.

To enable BOSS, the SDSS-III Collaboration undertook a major upgrade (largely funded by DOE) of the original SDSS spectrographs. The BOSS spectrograph followed the same basic design as SDSS, using aluminum plates supported in the telescope focal plane by aluminum cast cartridges. As with SDSS, plates are plugged manually with optical fibers that feed the two spectrographs mounted to the back of the primary mirror. The BOSS spectrograph was built with new optical elements and better CCDs to increase throughput and 50% more fibers (increased from 640 to 1000 per plate) to increase the overall sample size [12]. These upgrades allow BOSS to measure galaxy redshifts at fainter apparent magnitudes than the SDSS spectrographs, extending the redshift range of luminous galaxies to  $z \approx 0.7$ , increasing the galaxy density to three times the SDSS LRG sample to fully sample structure on the BAO scale, and covering an area of 10,000 deg<sup>2</sup>. Forecasts (described in [13] and [14]) predict BAO measurement precision from the full BOSS galaxy survey of 1.0% and 1.1% on  $D_A(z)$  for independent redshift bins centered at  $z = 0.35$  and  $z = 0.6$ , respectively. The forecast precision for  $H(z)$  at the same redshifts is 1.8% and 1.6%. BAO analysis of the Data Release 9 sample (DR9), about 1/3 the size of the final data set, yield 1.9% precision on the weighted combination  $(D_A^2/H)^{1/3}$  at  $z = 0.57$  [15]. Analyses that use the full shape of the galaxy power spectrum instead of isolating the BAO peak can sharpen the measurement precision by a significant factor and add constraints on neutrino masses and other cosmological parameters, at the price of relying more strongly on models of non-linear galaxy bias (e.g., [16]). Redshift-space distortion (RSD) analysis of the BOSS sample (e.g., [17]) has yielded the tightest constraints to date on the growth rate of structure and on cosmic geometry via the Alcock-Paczynski ([18]) effect.

BOSS is also pioneering a novel method of measuring BAO at high redshift using the 3-dimensional clustering of Ly $\alpha$  forest absorption towards a dense grid of high-redshift quasars ( $2.15 < z < 3.5$ ). Analyses of the DR9 data set have yielded BAO measurements at  $z \sim 2.5$  with precision of 2-3% [19, 20], the first BAO measurement by any method at  $z > 1$ . Because RSD strongly enhances line-of-sight clustering in the Ly $\alpha$  forest, the best constrained combination of  $H(z)$  and  $D_A(z)$  is heavily weighted towards  $H(z)$ , which is directly sensitive to the total energy density at the measurement redshift. Extrapolating to the size of the final BOSS data set implies an eventual measurement precision of 1.5% on a combination that is approximately  $D_A^{0.2}/H^{0.8}$ .

SDSS-III is being carried out by an international collaboration of several hundred scientists at 40+ institutions in the U.S., Europe, Asia, and South America. U.S. funding comes from the Alfred P. Sloan Foundation, the DOE Office of Science, the NSF, and the participating institutions.

BOSS has stayed on budget and on or ahead of schedule in hardware development, software development, and observations, and it remains on target to meet or exceed its original design goals. The DR10 data set became public in summer 2013, and papers analyzing galaxy and Ly $\alpha$  forest clustering in this data set are expected in the second half of 2013. BOSS will complete all of its observations before summer 2014; the final data release, including 1.3 million new galaxy redshifts and spectra of more than 160,000  $z > 2$  quasars, is planned for December 2014.

More information about BOSS can be found in

Dawson, K. S., Schlegel, D. J., Ahn, C. P., Anderson, S. F., Aubourg, É., Bailey, S., et al. 2013. The Baryon Oscillation Spectroscopic Survey of SDSS-III. *AJ* 145, 10. [14]

Eisenstein, D. J., Weinberg, D. H., Agol, E., Aihara, H., Allende Prieto, C., Anderson, S. F., et al., 2011. SDSS-III: Massive Spectroscopic Surveys of the Distant Universe, the Milky Way, and Extra-Solar Planetary Systems. *AJ* 142, 72 [13]

Anderson, L., Aubourg, E., Bailey, S., Bizyaev, D., Blanton, M., Bolton, A. S., et al., 2012. The clustering of galaxies in the SDSS-III Baryon Oscillation Spectroscopic Survey: baryon acoustic oscillations in the Data Release 9 spectroscopic galaxy sample. *MNRAS* 427, 3435 [15]

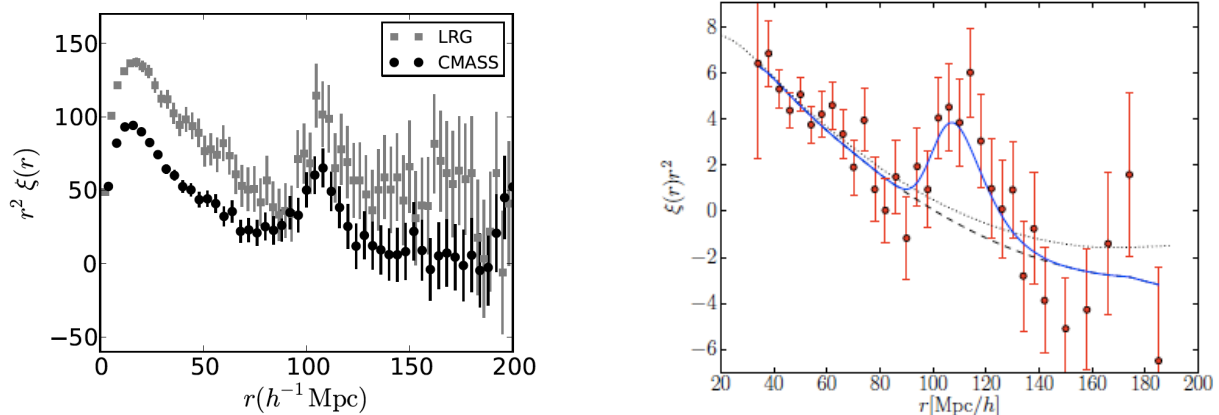


**Figure 1:** *Left:* The galaxy correlation function, multiplied by  $r^2$  to highlight large scales, from SDSS Luminous Red Galaxies (grey) at  $z = 0.35$  and BOSS galaxies (black) at  $z = 0.57$ . The amplitude of clustering is different because of the different galaxy types, but the BAO peak appears at the same comoving scale as expected. From [15]. *Right:* The correlation function of flux in the Ly $\alpha$  forest at  $z = 2.5$ , showing the BAO peak measured in intergalactic hydrogen absorption. From [20] (see also [19]).

### 3 The Dark Energy Survey (DES)

The Dark Energy Survey (DES) is using a powerful new instrument, the prime focus Dark Energy Camera on the Blanco 4-meter telescope at Cerro Tololo Inter-American Observatory (CTIO), to probe the origin of cosmic acceleration using Type Ia supernovae (SN), weak lensing (WL), galaxy clusters, and baryon acoustic oscillations (BAO) in photometric galaxy clustering. The 570-Megapixel DECam, equipped with 74 red-sensitive CCDs, has a 3 deg<sup>2</sup> field of view. The camera was commissioned in Sept.-Oct. 2012 following significant upgrades to the telescope and its control systems. Science verification observations took place in late 2012-early 2013, and the camera is performing to specifications. The survey proper began in August 2013 and will use 525 nights of observation over the ensuing five years.

DES will image 5000 deg<sup>2</sup> of the southern and equatorial sky in five optical passbands (*grizY*), reaching a depth of approximately 24th magnitude (AB) in each band. The imaging depth is about 2 magnitudes deeper than the SDSS, and the typical image quality is much better (0.9" seeing vs. 1.4"). The imaging survey will detect 300 million galaxies, with approximately 200 million WL shape measurements ( $n_{\text{eff}} \sim 11 \text{ arcmin}^{-2}$ ). This represents a roughly 40-fold improvement over the CFHTLenS WL survey [7], which is the largest that exists today, enabling far more powerful constraints on the growth of dark matter clustering and the cosmic expansion history. DES will cover the entire 2500 deg<sup>2</sup> footprint of the South Pole Telescope Sunyaev-Zel'dovich cluster survey, and it will detect clusters as enhancements of optical galaxy counts over its entire footprint, with  $\sim 10^5$  clusters of mass  $M \geq 10^{14} M_{\odot}$  expected over the full survey area. Even more crucial for cluster-based studies of dark energy, DES will enable stacked weak lensing measurements (e.g., [21]) of the virial masses and extended mass profiles of clusters detected in optical, SZ, or X-ray catalogs, sharply reducing the mass-calibration uncertainties that are the limiting systematic of this technique. Large scale clustering of galaxies in bins of photometric redshift will enable BAO measurements of the angular diameter distance  $D_A(z)$  out to  $z \sim 1.4$ , as well as constraints on neutrino masses and primordial non-Gaussianity.

The DES supernova search will cover 30 deg<sup>2</sup> in *griz*, returning to each field on a  $\sim 5$ -day cadence throughout each DES observing season. Forecasts based on detailed simulations [22] indicate that DES will discover and measure high-quality light curves for approximately 4000 Type Ia SNe over the redshift range  $0.5 < z < 1.2$ , roughly a factor of ten more than the Supernova Legacy Survey (SNLS). About 20% of these will be followed up with real-time spectroscopy from other telescopes, while spectroscopic host galaxy redshifts will be obtained for a larger fraction of the SNe on a longer timescale.

The statistical precision of DES SN, WL, cluster, and photometric galaxy clustering measurements will far exceed those of any imaging surveys that exist today. Forecasts for dark energy observables depend on assumptions about the systematic errors that can be achieved with DES data. The SN survey has very small statistical uncertainties over nearly its full redshift range, so it will likely be limited by systematic uncertainties in photometric calibration, reddening and extinction corrections, and evolution of the supernova population. These are already the limiting factors in current SN studies (e.g., [6]), but the much larger numbers in DES will allow selection of and cross-checks among multiple subsets of SNe defined by light curve shape, color, and host galaxy properties, thus enabling tighter control of systematics. Photometric calibration errors will be controlled in part by repeated measurements of the system throughput and through real-time monitoring of precipitable water vapor at the site. For BAO one can forecast the errors on  $D_A(z)$  in bins of photometric redshift, finding expected precision of 1.5-2.5% [23]. SN and BAO measurements at the same redshift have complementary information content because the SN distance scale is calibrated in the Hubble flow while the BAO distance scale is calibrated in absolute units based on cosmological parameters determined by CMB data — in effect, SN distances are in  $h^{-1}$  Mpc and BAO distances in Mpc, where  $h \equiv H_0/100 \text{ km s}^{-1} \text{ Mpc}^{-1}$  is the Hubble parameter.

Cluster and WL analyses are sensitive to both geometry and structure growth, but one can characterize their sensitivity by considering a constrained model in which the overall amplitude of matter clustering is the only free parameter. Scaling from forecasts in [1] implies that  $M \geq 10^{14} M_{\odot}$  clusters calibrated by stacked weak lensing in DES can constrain the matter clustering amplitude (proportional to  $\sigma_8$ ) with 1-2% precision and approximately independent errors in  $\Delta z = 0.1$  redshift bins from  $z \approx 0.2$  to  $z \approx 1$ , with an aggregate precision better than 0.5% (see their figure 30). Cosmic shear measurements with  $N_{\text{eff}} = 2 \times 10^8$  could in principle achieve aggregate precision of 0.2% or better on the matter clustering amplitude if limited purely by galaxy shape noise, but marginalizing over uncertainties in shear calibration, photometric redshifts, and intrinsic alignments may lead to larger errors.

DES is being carried out by an international collaboration of more than 200 scientists, with member institutions in the U.S., the U.K., Spain, Brazil, Germany, and Switzerland. U.S. funding is being provided by the DOE Office of Science, the NSF, and the participating institutions.

More information about DES can be found in

<https://www.darkenergysurvey.org/reports/proposal-standalone.pdf>

Bernstein, J. P., Kessler, R., Kuhlmann, S., Biswas, R., Kovacs, E., Aldering, G. et al. 2012, Supernova Simulations and Strategies for the Dark Energy Survey, *ApJ*, 753, 152

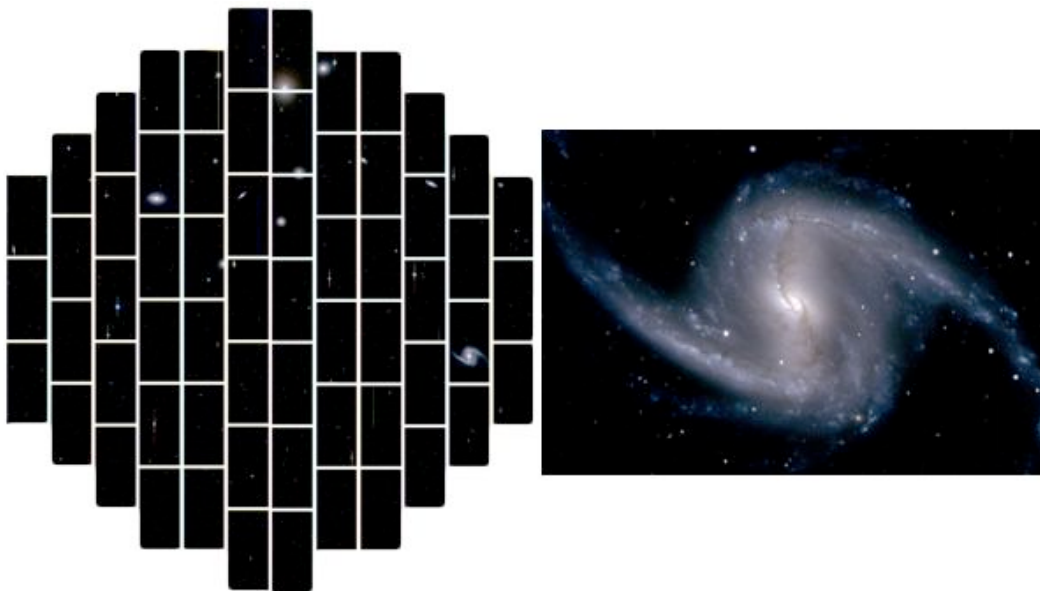


**Figure 2:** First light images of the nearby Fornax galaxy cluster from the 570-Megapixel Dark Energy Camera at CTIO. The left panel shows the full field of view of the 72-CCD camera. The right panel zooms in on the image of the galaxy NGC 1365.

## 4 The Extended Baryon Oscillation Spectroscopic Survey (eBOSS)

While BOSS will complete its observations in 2014, the Sloan Telescope and BOSS spectrographs will likely remain the most powerful facility for wide field spectroscopic surveys until the commissioning of the Dark Energy Spectroscopic Instrument (DESI, projected for 2018). Approved as a major cosmology survey in SDSS-IV (2014–2020), eBOSS will capitalize on this premier facility with spectroscopy on a massive sample of galaxies and quasars in the relatively uncharted redshift range that lies between the BOSS galaxy sample and the BOSS Ly $\alpha$  sample. The targets for eBOSS spectroscopy will consist of: Luminous Red Galaxies (LRGs:  $0.6 < z < 0.8$ ) at a density of  $50 \text{ deg}^{-2}$ , Emission Line Galaxies (ELGs:  $0.6 < z < 1.0$ ) at a density of  $180 \text{ deg}^{-2}$ , “clustering” quasars to directly trace large-scale structure ( $1 < z < 2.2$ ) at a density of  $90 \text{ deg}^{-2}$ , re-observations of faint BOSS Ly $\alpha$  quasars ( $2.2 < z < 3.5$ ) at a density of  $8 \text{ deg}^{-2}$ , and new Ly $\alpha$  quasars ( $2.2 < z < 3.5$ ) at a density of  $12 \text{ deg}^{-2}$ .

The new target selection for eBOSS has already been proven in a series of commissioning observations taken with the BOSS spectrograph in 2013. As shown in those commissioning observations, all target classes will satisfy classification efficiencies better than 80% using the same effective exposure times as BOSS. Quasars and LRGs will be observed over  $7500 \text{ deg}^2$  ( $5000 \text{ deg}^2$  for Ly $\alpha$  quasars) and will be the primary primary focus of the program. The ELG targets will provide a BAO constraint comparable to the DR9 BOSS galaxy results over a  $1500 \text{ deg}^2$  area.

Using the techniques for BAO analysis developed in BOSS, eBOSS will measure both the distance-redshift relation and the evolution of the Hubble parameter  $H(z)$  with these new density tracers, resulting in the first BAO measurements at  $1 < z < 2.2$ . The wide redshift range of the eBOSS tracers will disentangle the evolution of structure growth from the amplitude of clustering, thus providing new constraints on GR through RSD analyses. The expected constraints from BAO and RSD are shown in the table below, where the fractional distance error from BAO is parametrized by an optimal combination of  $D_A(z)$  and  $H(z)$  denoted by a generalized distance parameter “R” and the growth of structure from RSD is parametrized by  $f\sigma_8$ , the product of the matter fluctuation amplitude  $\sigma_8$  and the growth rate  $f \equiv d \ln \sigma_8 / d \ln a$ .

Because the large volume of eBOSS will capture many large-scale modes, measurements of the matter power spectrum will impose important new constraints on non-Gaussian primordial fluctuations in the early universe and on neutrino masses. Given Planck results, BAO measurements from BOSS and eBOSS, 5%  $H_0$  priors, and an assumption of zero curvature, predictions from eBOSS imply a 95% upper limit  $\sum m_\nu < 0.104$  when combining the results from the eBOSS LRGs, ELGs and quasars. The upper limit on neutrino masses derived from eBOSS will be comparable to the minimum allowed mass in an inverted hierarchy. Assuming a baseline from Planck measurements and a 5%  $H_0$  constraint, primordial non-gaussianities of the local form can be constrained to a precision  $\sigma_{f_{nl}} = 12$  (68% confidence) by the combination of eBOSS LRG, ELG, and quasars.

**Table 0-1.** Basic parameters expected for each eBOSS sample, together with predictions for the effective volumes and fractional constraints on BAO distance measurements and growth of structure.

Sample	$N_{\text{target}}$	purity	$\bar{n}_{\text{peak}} (h^{-1}\text{Mpc})^{-3}$	$V_{\text{eff}} \text{ Gpc}^3$	$\sigma_R/R$	$\sigma_{f\sigma_8}/f\sigma_8$
LRGs $0.6 < z < 0.8$	375,000	95%	$1.4 \times 10^{-4}$	4.5	0.009	0.029
ELGs $0.6 < z < 1$	270,000	80%	$3.4 \times 10^{-4}$	2.1	0.018	0.035
Quasars $1 < z < 2.2$	675,000	70%	$0.21 \times 10^{-4}$	4.4	0.020	0.036
BOSS LyA Quasars	160,000	—	—	—	0.015	—
BOSS + eBOSS LyA Quasars	310,000	70%	—	—	0.011	—

SDSS-IV is being carried out by an international collaboration with member institutions in the U.S., Europe, Asia, and South America.

More information about SDSS-IV and eBOSS can be found at

<http://www.sdss3.org/future/sdss4.pdf>

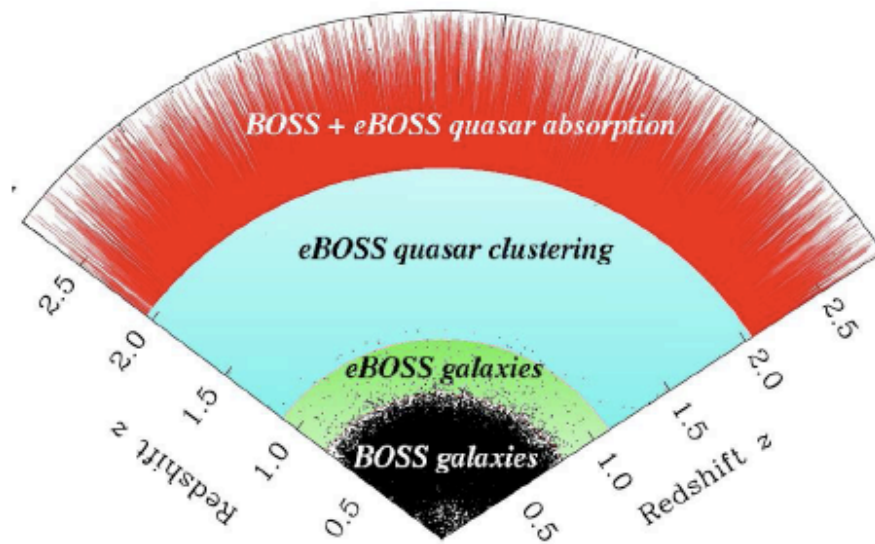


**Figure 3:** Complementarity of the eBOSS and BOSS redshift ranges for BAO measurements. Black dots show a slice through the distribution of BOSS galaxies, with maximum redshift  $z \approx 0.7$ . eBOSS luminous galaxies and emission line galaxies will probe the redshift range  $0.6 < z < 1.1$ . eBOSS quasars will yield the first percent-level BAO measurements in the redshift range  $1 < z < 2$ . At  $z > 2$ , the addition of eBOSS quasar spectra to BOSS spectra will sharpen the precision of BAO measurements from the Ly $\alpha$  forest.

## 5 The Hobby-Eberly Telescope Dark Energy Experiment (HETDEX)

The Hobby-Eberly Telescope Dark Energy Experiment (HETDEX) will measure the expansion rate of the universe in the redshift range  $1.9 < z < 3.5$ , using Ly $\alpha$  emitting galaxies (LAEs). HETDEX consists of a significant upgrade to the 10-meter Hobby-Eberly Telescope (HET), a new spectroscopic instrument called VIRUS, and a significant observing campaign. The upgrade is currently in progress and on schedule for completion mid-2014. The VIRUS instrument consists of 33,500 optical fibers feeding 75 pairs of spectrographs, providing a wavelength coverage of 350-550nm with a resolving power of 750. The survey is blind, requiring no pre-selection of the targets.

The main HETDEX survey will cover 300 square degrees at a high-declination field with a 20% fill factor. Thus, about 60 square degrees of sky will be covered with spectra. The main survey will produce about 0.7 million LAEs over  $1.9 < z < 3.5$ , about 1.0 million [OII] emitters at  $z < 0.5$ , and significant numbers (many 100,000) of quasars, stars, and galaxies. The main survey will take three observing seasons to complete, and thus will run from 2014 to 2017.

HETDEX will also have an equatorial field with a footprint of 150 square degrees and 30 square degrees of sky with spectra. The equatorial field will take three observing seasons to complete, and will run from 2014 to 2017. There are plans for extensions of both the high-dec and equatorial fields in order to increase the full survey volume by a factor of two over the main survey. The survey extensions will require an additional two years to complete.

Forecasts indicate that the main HETDEX survey will produce a measure of  $H(z = 2.3)$  to 0.95% and a measure of  $D_A(z = 2.3)$  to 0.95%. The combined distance measure ( $\sigma_R$ ) will have an accuracy of 0.85%. Including both the equatorial and extension fields will increase the precision on each of these quantities by about 30%, but we report the numbers above from the main HETDEX survey as a conservative estimate. The decision on whether to have the extension field will be made after the first two years of the HETDEX survey.

HETDEX will also produce a measure of growth of structure. The main survey will measure  $f\sigma_8$  to an accuracy of 2% at  $z = 2.3$ . As above, inclusion of the equatorial and extension fields will improve the precision by about 30%.

More information about HETDEX can be found at

<http://hetdex.org>

## 6 The Subaru Hyper-Suprime Camera and Prime Focus Spectrograph

The Subaru 8.2-meter telescope at Mauna Kea, Hawaii has a unique prime focus located 15 m above the primary mirror. The use of this prime focus enables a wide field of view ( $\sim 1.7 \text{ deg}^2$ ), exploited first by the Suprime-Cam instrument. Using this instrument, the high mechanical and optical quality of the Subaru telescope have been demonstrated. This camera is now being replaced by a more potent instrument, the Hyper Suprime-Cam (HSC). This new camera has been built by National Astronomical Observatory of Japan (NAOJ) and the Kavli Institute for the Physics and Mathematics of the Universe (KIPMU) in collaboration with international academic and industrial partners. This instrument and its 116 CCD camera now being commissioned on the Subaru telescope will enable a wide and deep optical survey scheduled to start from early 2014. This survey should deliver deep imaging of about  $1,500 \text{ deg}^2$  in five bands (*grizy*) with magnitude limits of 26 and 24 in the *i* and *y* band ( $5\sigma$ , for a point source in 2 arcsec diameter aperture), respectively.

The benefits of devising a multi-object spectrometer sharing the optics designed for HSC became quickly apparent and led to the Subaru Prime Focus Spectrograph (PFS) project. PFS is designed to allow simultaneous spectroscopy of 2400 astronomical targets over a 1.3 degree hexagonal field. It shares the Wide Field Corrector and associated Field Rotator and Hexapod already constructed for the HSC. An array of 2400 optical fibers is in the Prime Focus Instrument and each fiber tip position is controlled in-plane by a two-stage piezo-electric Fiber Positioner Cobra system. Each fiber can be positioned within a particular patrol region such that these patrol regions fully sample the 1.3 deg field. A Fiber Connector relays light to four identical fixed-format 3-arm twin-dichroic all-Schmidt Spectrographs providing continuous wavelength coverage from 380nm to 1.3 $\mu$ m. The blue and red channels will use two Hamamatsu 2K4K edge-buttable fully-depleted CCDs (as in HSC). The near-infrared channel will use a new Teledyne 4RG 4K4K HgCdTe 1.7 $\mu$ m cut-off array.

This instrument will be used to observe the same footprint as the HSC survey. The union of the HSC and PFS survey is known as the Subaru Measurement of Images and Redshifts (SuMIRE) project. This optical/near-infrared multi-fiber spectrograph targets will lead to unique cosmological measurements based on the clustering of galaxies, but also studies of galactic archeology and of the evolution of galaxies throughout cosmic time. Before and during the era of extremely large telescopes, PFS will be able to obtain 2400 cosmological/astrophysical targets simultaneously with an 8-10 meter class telescope.

The PFS collaboration, led by IPMU, consists of USP/LNA in Brazil, Caltech/JPL, Princeton, and JHU in USA, LAM in France, ASIAA in Taiwan, and NAOJ/Subaru.

More information about the Subaru HSC, PFS, and SuMIRE can be found at

Takada, M., Ellis, R., Chiba, M., et al., arXiv:1206.0737v2

<http://sumire.ipmu.jp>

<http://sumire.ipmu.jp/en/2652>

<http://www.naoj.org/Projects/HSC/index.html>

## 7 The Dark Energy Spectroscopic Instrument (DESI)

DESI, the Dark Energy Spectroscopic Instrument, will be a major leap forward in capability for wide-field spectroscopy and a powerful experiment for the Cosmic Frontier research program. DESI is a multi-fiber spectroscopic instrument that will be installed on the Mayall 4-m telescope to enable massively parallel measurements of galaxy redshifts. The resulting 3D map of the Universe will enable baryon acoustic oscillation (BAO) measurements to chart the expansion history of the Universe, as well as redshift space distortion measurements to chart the growth of structure. DESI fits perfectly within the established Cosmic Frontiers Dark Energy program: as a Stage-IV BAO experiment, it complements the DES and LSST imaging surveys, whose strengths are weak lensing and Type Ia supernovae, and it fills the hiatus between the end of the DES survey and the start of LSST. CD-0 (mission need) was awarded by DOE in September 2012, CD-1 (conceptual design) is scheduled for January 2014, and first light is planned in 2018. LSST and DESI in combination will satisfy the four Stage IV dark energy probes as established by the Dark Energy Task Force. The DESI collaboration is currently represented by 160 scientists from 50 institutions in the U.S., Australia, Brazil, China, France, Germany, Korea, Mexico, Spain, Switzerland and the U.K..

Performing a wide, deep spectroscopic redshift survey of 20 to 30 million galaxies over  $14,000 - 18,000 \text{ deg}^2$  in a five-year survey requires a high throughput spectrograph capable of observing thousands of spectra simultaneously. The new instrument will be installed on the Mayall Telescope operated at Kitt Peak, Arizona. A key DESI innovation is a new prime focus corrector optic creating an 8 square degree field of view. Optical fibers transport the galaxy light from the focal plane to the spectrographs. The fiber tips are placed with high accuracy using robotic positioners, and the entire focal plane is reconfigured for each exposure in less than a minute. The redshifts of 5000 galaxies are measured with each 20-minute exposure. The fiber optical cables are split into ten separate bundles of 500 fibers. Each bundle then travels 40 meters from the focal plane to a 500-fiber slit array feeding (ten) separate spectrographs. The full spectral bandpass is 360 to 980 nm divided by dichroics between three arms, attaining a resolution as high as  $R = 5200$ .

DESI will use a combination of emission-line galaxies (ELGs), luminous red galaxies (LRGs), and quasars to trace large scale structure out to redshift  $z \approx 1.7$  and Ly $\alpha$  forest absorption towards nearly one million high-redshift quasars to measure BAO at redshifts  $1.9 < z < 4$ . As detailed in the Table below, forecast BAO errors on the distance scale are 0.35 – 1.1% per  $\Delta z = 0.2$  redshift bin out to  $z = 1.7$ , with an aggregate precision of 0.17%. Typical distance errors per bin from the Ly $\alpha$  forest, augmented by cross-correlations with quasar density, are  $\sim 1\%$ , with an aggregate precision of 0.37%. Structure growth is measured via redshift-space distortions in the galaxy and quasar distributions, with per-bin errors on the parameter combination  $f\sigma_8$  below 2% over the range  $0.2 < z < 1.6$  and aggregate precision of 0.35%. The forecasts here use the methods of [24] for BAO distance and [25] for RSD, where the RSD uses comoving wavenumbers with  $k < 0.2 h \text{ Mpc}^{-1}$  and bias factors are assumed to follow  $b(z) = b_0 (D(z=0)/D(z))$ , where  $b_0 = 1.7, 0.84$ , and 1.2 for LRGs, ELGs, and QSOs, respectively.

In addition to the measurement of the expansion history of the Universe and the growth rate of large-scale structure, DESI has an enormously broad scientific reach. As one example, DESI will provide an important constraint on the sum of neutrino masses, one that is complementary to other approaches that can determine the mass hierarchy or establish the neutrino mass scale. Power spectrum measurements by DESI are sensitive to the sum of neutrino masses. Because one of the splittings of the squares of the neutrino mass is about  $2.43 \times 10^{-3} \text{ eV}^2$  [KamLAND Collaboration, 2005], we know that at least one neutrino has a mass of at least 0.05 eV. If neutrinos have an inverted mass hierarchy, the minimum sum of the neutrino masses is roughly twice this (since the other splitting is considerably smaller). The 1- $\sigma$  limits obtained on the sum of neutrino masses should be 0.024 eV (integrating in k-space up to  $k_{\text{max}} = 0.1 h \text{ Mpc}^{-1}$ ). More stringent constraints (rms of 0.017 eV) are possible if non-linearities are controlled up to  $k_{\text{max}} = 0.2 h \text{ Mpc}^{-1}$ .

More information about DESI, and the prior proposals BigBOSS and DESpec can be found in:

Levi, M., et al., 2013, The DESI Experiment, a whitepaper for Snowmass 2013, arXiv:1307.0000.

Schlegel, D., et al., 2011, The BigBOSS Experiment, arXiv:1106.1706.

Abdalla, F., et al., 2012, The Dark Energy Spectrometer (DESPEC), arXiv:1209.2451.

$z$	$\frac{\sigma_{R/s}}{R/s}$ %	$V$ Gpc <sup>3</sup>	$\frac{dN_{ELG}}{dz \text{ ddeg}^2}$	$\frac{dN_{LRG}}{dz \text{ ddeg}^2}$	$\frac{dN_{QSO}}{dz \text{ ddeg}^2}$	$\frac{\sigma_{f\sigma_8}}{f\sigma_8}$ %
0.1	1.77	0.81	358	38	5	3.26
0.3	0.82	4.72	368	126	22	1.60
0.5	0.56	10.33	237	333	31	1.34
0.7	0.41	16.08	709	570	34	0.94
0.9	0.36	21.17	1436	442	44	0.77
1.1	0.42	25.31	1393	13	56	0.80
1.3	0.41	28.51	1444	0	69	0.81
1.5	0.51	30.87	802	0	81	1.04
1.7	1.10	32.52	152	0	80	2.36

Constraint forecasts for DESI, courtesy of P. McDonald.

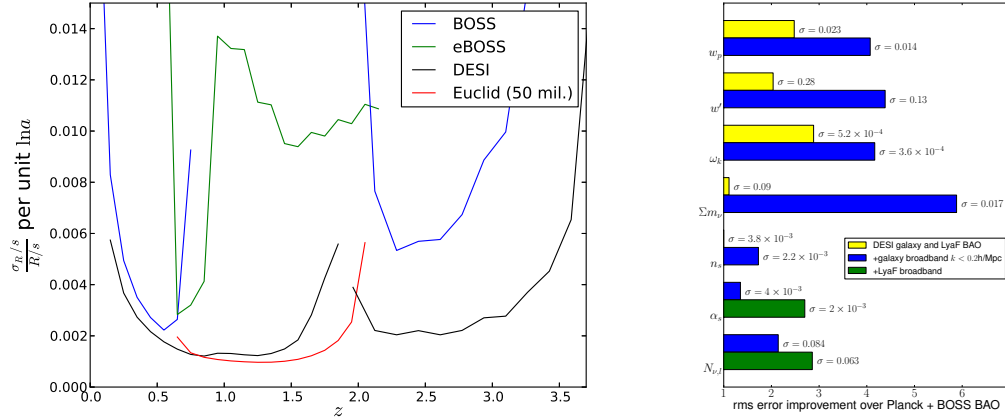


**Figure 4:** *Left:* (a) Fractional error on the BAO distance scale (isotropic dilation factor), as a function of redshift, *per unit*  $\ln(a)$  (in other words, the effect of any arbitrary redshift bin width  $\Delta z$  is removed in this plot). Errors from the Ly $\alpha$ F measurement, which dominate at  $z > 1.8$ , are computed following [26], with a modest but significant additional contribution from cross-correlations with quasar density. We assume 50 million galaxies for Euclid. *Right:* (b) Improvement in parameters over Planck (final projection, including polarization) plus BOSS BAO. Yellow bars show the improvement with DESI BAO, including Ly $\alpha$ F. Blue bars show the additional improvement when optimistic broadband power is used, with  $k < 0.2 h \text{ Mpc}^{-1}$ . Green additionally adds potential constraints from broadband (including small-scale 1D) Ly $\alpha$ F power. Dark energy parameters are defined by the equation of state  $w(z) = w_p + (a_p - a)w'$ , where  $a_p$  is chosen to make the errors on  $w_p$  and  $w'$  independent.  $\omega_k \equiv \Omega_k h^2$  is the equivalent physical density of curvature.  $\Sigma m_\nu$  is the sum of masses of neutrinos, in eV.  $\alpha_s$  and  $n_s$  parameterize the inflationary perturbation power spectrum, i.e.,  $P_{\text{inflation}}(k) \propto k^{n_s + \frac{1}{2}\alpha_s \ln(k/k_*)}$ .

## 8 Large Synoptic Survey Telescope

The Large Synoptic Survey Telescope (LSST) is a wide-field, ground-based telescope, designed to image a substantial fraction of the sky in six optical bands every few nights. It is planned to operate for a decade allowing the stacked images to detect galaxies to redshifts well beyond unity. The LSST and the survey are designed to meet the requirements of a broad range of science goals in astronomy, astrophysics and cosmology, including the study of dark energy. The LSST was the top-ranked large ground-based initiative in the 2010 National Academy of Sciences decadal survey in astronomy and astrophysics.

The Dark Energy science goals of LSST are:

- Weak gravitational lensing: the detection of light from distant sources due to the bending of space-time by baryonic and dark matter along the line of sight. Tomographic measurements of weak lensing will provide percent-level constraints on cosmological parameters.
- Large-scale structure: the large-scale power spectrum for the spatial distribution of matter as a function of redshift. This includes the Baryonic Acoustic Oscillations and the measurement of the distance-redshift relation. With the enormous number of galaxies detected by LSST, the co-moving distance will be measured with percent-level precision.
- Type Ia Supernovae: luminosity distance as a function of redshift measured with Type Ia SNe as standardizable candles. LSST will discover and measure at least 500 SNe Ia per season, giving tens of thousands of well-measured SNe Ia light curves up to  $z \sim 1$  over the full ten-year survey.
- Galaxy clusters: the spatial density, distribution, and masses of galaxy clusters as a function of redshift. LSST will be able to measure the masses of  $\sim 20,000$  clusters to a precision of 10%.
- Strong gravitational lensing: the angular displacement, morphological distortion, and time delay for the multiple images of a source object due to a massive foreground object. LSST will give a sample of  $\sim 2600$  time-delayed lensing systems, an increase of  $100\times$  compared to the sample available today.

The observatory will be located on Cerro Pachon in northern Chile (near the Gemini South and SOAR telescopes), with first light expected around 2019. The survey will yield contiguous overlapping imaging of over half the sky in six optical bands (*ugrizy*, covering the wavelength range 320-1050 nm). The LSST camera provides a 3.2 Gigapixel at focal plane array, tiled by 189 4kx4k CCD science sensors with  $10\mu\text{m}$  pixels. This pixel count is a direct consequence of sampling the  $9.6\text{ deg}^2$  field-of-view (0.64m diameter) with  $0.2\times 0.2\text{ arcsec}^2$  pixels (Nyquist sampling in the best expected seeing of  $\sim 0.4\text{ arcsec}$ ). The observing strategy for the main survey will be optimized for homogeneity of depth and number of visits. The current baseline design will allow about  $20,000\text{ deg}^2$  of sky to be covered using pairs of 15-second exposures in two photometric bands every three nights on average, with typical  $5\sigma$  depth for point sources of  $r \sim 24.5$ . The system will yield high image quality as well as superb astrometric and photometric accuracy for a ground-based survey. The coadded data within the main survey footprint will have a depth of  $r \sim 27.5$ . 10% of observing time will be used to obtain improved coverage of parameter space, such as very deep ( $r \sim 26$ ) observations taken over the course of an hour, optimized for detection of faint SNe.

Historically, our understanding of the cosmic frontier has progressed in step with the size of our astronomical surveys, and in this respect, LSST promises to be a major advance: its survey coverage will be approximately ten times greater than that of the Stage III Dark Energy Survey. The dark energy constraining power of LSST could be several orders of magnitude greater than that of a Stage III survey [27]. LSST will go much further than any of its predecessors in its ability to measure growth of structure, and will provide a stringent test of theories of modified-gravity.

While these projections for LSST statistical significance are compelling, they probably do not capture the true nature of the revolution that LSST will enable. The sheer statistical power of the LSST dataset will allow for an all-out attack on systematics, using a combination of null tests and hundreds of nuisance parameters and by combining probes.

Beyond tests of systematics, there is a growing sense in the community that the old, neatly separated categories of dark energy probes will not be appropriate for next generation surveys. For example, instead of obtaining constraints

on dark energy from cluster counts and cosmic shear separately, LSST scientists may use clusters and galaxy-galaxy lensing simultaneously to mitigate the twin systematics of photometric redshift error and mass calibration [28]. A homogeneous and carefully calibrated dataset such as LSST's will be essential for such joint analyses.

More information on LSST can be found in the following LSST overview papers and the Science Requirements Document:

Ivezić, Z., Tyson, J., Allsman, R., Andrew, J., & Angel, R., et al., 2008. LSST: from Science Drivers to Reference Design and Anticipated Data Products. 0805.2366 [29].

Abell, P and the LSST Science Collaborations, 2009, LSST Science Book. 0912.0201 [30].

Abate, A. and the LSST Dark Energy Science Collaboration, 2012, Large Synoptic Survey Telescope Dark Energy Science Collaboration. 1211.0310 [31].

Ivezić, Z., & the LSST Science Collaboration, 2011, Large Synoptic Survey Telescope (LSST) Science Requirements Document. <http://www.lsst.org/files/docs/SRD.pdf>

## 9 Euclid

Euclid is a dark energy satellite mission scheduled for launch in the second quarter of 2020 [32]. Euclid is a European Space Agency (ESA) Medium Class mission in the Cosmic Vision program. ESA will provide the spacecraft, the 1.2m telescope, and launch on a Russian Soyuz from Kourou in French Guiana. The  $\sim 1200$  member Euclid Consortium (EC) will provide two instruments, a visible imager (VIS) and a near infrared spectrometer/photometer (NISP), data processing, and science analysis. ESA and the EC will jointly provide an archive to serve the data to the community.

Euclid is designed for two complementary dark energy probes. Euclid will perform a  $15,000 \text{ deg}^2$  weak gravitational lensing survey in a single wide optical filter. The surface density of resolved galaxies will be between 30 and 40 per square arcminute. This high surface density is enabled by the small PSF afforded via space-based, near diffraction limited observations. Photometric redshifts for the Euclid weak lensing galaxies will be measured from a combination of ground-based photometry from various sources and  $15,000 \text{ deg}^2$  near-infrared (NIR) 3 band (1-2 micron) photometric survey taken with Euclid’s NISP instrument. Euclid will also conduct a  $15,000 \text{ deg}^2$  spectroscopic survey aimed at galaxy clustering (BAO and RSD). Euclid will use the NISP grism to measure 50 million redshifts with an accuracy of  $\delta z < 0.001(1+z)$ . In addition to Euclid’s wide photometric and spectroscopic survey, it will perform a 40 square degree deep survey that reaches 2 magnitudes deeper (in both the optical and NIR) than the wide survey.

The aforementioned surveys, performed over 6.25 years in the ultra-stable environment available at the Earth-Sun L2 Lagrange point, will allow Euclid to address four primary science goals:

- Measure the equation-of-state of dark energy to high precision, using both expansion history and structure growth
- Measure the rate of structure growth to distinguish General Relativity from modified-gravity theories
- Test the Cold Dark Matter paradigm for structure formation, and measure the sum of the neutrino masses to a precision better than 0.02eV (when combined with Planck)
- Greatly improve constraints on cosmological initial conditions (relative to Planck data alone) to sharpen tests of inflation models or alternative theories of early-universe physics.

Detailed quantitative forecasts for Euclid performance on each of these goals can be found in [32]. Additionally, the Euclid data set of billions of galaxies morphologies and star formation rates out to  $z \sim 2$  and tens of millions of redshifts will form a rich legacy for the study of a wide range of cosmological and astrophysical phenomena.

Euclid’s VIS instrument contains 36  $4\text{k} \times 4\text{k}$  e2v CCDs and covers 0.5 square degrees at a pixel scale of  $0.1''$  per pixel. This instrument has a single, broad RIZ filter. A dichroic allows simultaneous operation with the NISP instrument, which can operate in either imaging or grism spectroscopy mode. The NISP contains 16  $2\text{k} \times 2\text{k}$  Teledyne H2RG detectors. In imaging mode, there are three filters (Y,J,H) and in slitless spectroscopy mode there are two grisms and two filters, providing a spectral resolution of  $\frac{\lambda}{\delta\lambda} \sim 250$  over 2 pixels.

Euclid data will be released via an archive after a proprietary period. The current plan, not yet finalized, has three major data releases: release of the first year of data (about  $2500 \text{ deg}^2$ ) 26 months after the start of the survey, a release of  $7500 \text{ deg}^2$  two years later, and a final release containing all of the Euclid data three years after that.

There is already significant involvement in Euclid by US-based scientists. During the Euclid development phase LBNL (DOE) gave support to the Euclid Consortium’s efforts to define the NISP architecture in exchange for 7 LBNL scientists to join the EC, and LBNL was given a non-voting membership on the EC’s governing Euclid Consortium Board. There were also 7 US scientists who were granted EC membership due to their involvement in Euclid from its inception. In 2013, NASA officially joined Euclid by providing 20 “triplets” (16 flight and four spares), which consist of a characterized H2RG detector, a cryogenic cable, and cold readout electronics. In exchange for this hardware contribution to NISP, NASA was allowed to select 40 US investigators to become EC members, and NASA was granted a voting member of the Euclid Consortium Board and a seat on the 13-member ESA Euclid Science Team.

More information about Euclid can be found in

Euclid Definition Study Report, Laureijs, R., Amiaux, J., Arduini, S., et al. 2011, arXiv:1208.3369 [32]

<http://sci.esa.int/science-e/www/area/index.cfm?fareaid=100>

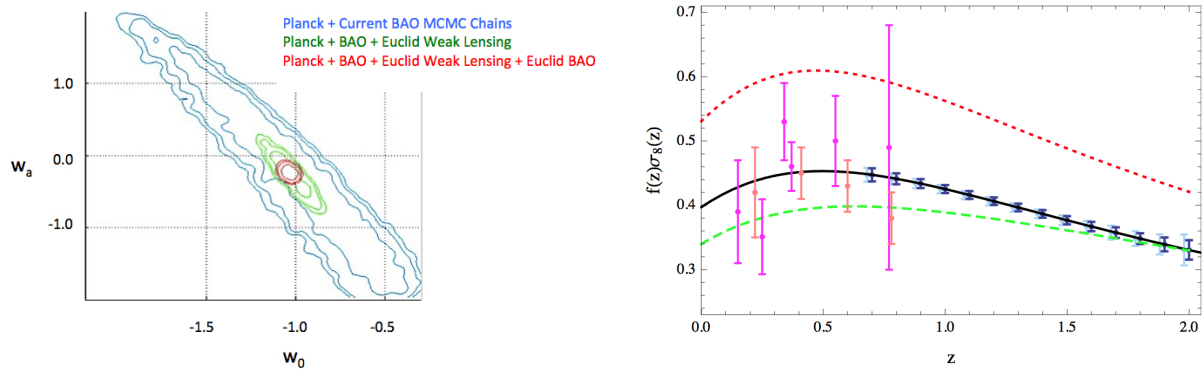


**Figure 5:** *Left:* Projected constraints on parameters of the dark energy equation of state for combinations of Planck CMB data with current BAO measurements (blue), adding projected Euclid WL measurements (green), and adding projected Euclid WL and BAO measurements (red). Modeling details are given in [32], though this figure (courtesy of the Euclid Consortium) uses updated performance estimates. *Right:* Constraints on the structure growth parameter combination  $f(z)\sigma_8(z)$ , comparing projections for Euclid redshift-space distortion measurements (blue) to existing constraints from the WiggleZ survey (orange) and earlier studies (magenta). Figure from [33].

## 10 The Wide Field Infrared Survey Telescope (WFIRST)

The Astro2010 Decadal Survey of astronomy recommended a Wide Field Infrared Survey Telescope as its top ranked priority for a large space mission, recognizing that improvements in infrared detector technology enabled a mission that would achieve dramatic advances across a wide range of astrophysics. Pinning down the properties of dark energy is one of the primary science goals of WFIRST, and its design builds heavily on earlier plans for a DOE-NASA Joint Dark Energy Mission (JDEM), which in turn built on DOE’s proposed SuperNova Acceleration Probe (SNAP). Following Astro2010, NASA commissioned a Science Definition Team (SDT) to develop a detailed plan for WFIRST. The design reference mission (DRM1) described in the SDT’s final report [34] uses a 1.3m unobstructed telescope and an infrared camera with a  $0.375 \text{ deg}^2$  field of view for imaging and slitless spectroscopy. More recently, a new SDT assessed an implementation of WFIRST using one of the Hubble-quality, 2.4m telescopes offered to NASA after the discontinuation of the national security program for which they were originally built. This implementation, known as WFIRST-AFTA (or informally as WFIRST-2.4), appears the most likely to go forward, so it is the one we describe here.

As described in the SDT report [35], WFIRST-AFTA would use a 300-megapixel IR camera with 0.11-arcsec pixels and a  $0.281 \text{ deg}^2$  field of view. In the 6-year prime mission, 1.9 years is devoted to a high-latitude imaging and spectroscopic survey of  $2000 \text{ deg}^2$ , and 0.5 years to a supernova survey with three different tiers of area and redshift. The high-latitude imaging survey will measure weak lensing shapes of  $\approx 500$  million galaxies in three bands (roughly J, H, and a shortened K) and weak lensing mass profiles of 40,000 massive ( $M > 10^{14} M_{\odot}$ ) clusters. The spectroscopic survey will measure H $\alpha$  emission-line redshifts of 20 million galaxies at  $z = 1 - 2$  and 2 million [OIII] emission-line galaxies at  $z = 2 - 3$ . The supernova survey will detect, monitor, and spectroscopically confirm 2700 Type Ia supernovae over the redshift range  $z = 0.1 - 1.7$ . With the assumptions described by [35], the forecast aggregate measurement precision from these surveys is:

- SN distance: 0.20% at  $z < 1$ , 0.34% at  $z > 1$
- BAO  $D_A(z)/H(z)$ : 0.40%/0.72% at  $z = 1 - 2$ , 1.3%/1.8% at  $z = 2 - 3$
- Growth constraints from WL/clusters: 0.16%/0.14% at  $z < 1$ , 0.54%/0.28% at  $z > 1$ ; also 1.2% from RSD at  $z = 1 - 2$

These measurements in turn enable stringent tests of dark energy and modified gravity models.

As a dark energy mission, WFIRST-AFTA complements Euclid in several ways. The large aperture and IFU spectrometer on WFIRST-AFTA make it an ideal facility for supernova cosmology; this is an important probe for WFIRST-AFTA that is not incorporated in the current Euclid plan. The WFIRST-AFTA galaxy redshift survey is “narrow-deep” compared to Euclid’s “shallow-wide”; while the total number of galaxies is similar and the forecast BAO precision comparable, the average space density in the WFIRST-AFTA is an order of magnitude higher, enabling techniques that make more use of small scale clustering or higher order statistics. The Euclid WL survey is designed for maximum statistical power, while the WFIRST-AFTA strategy has a much higher level of redundancy for internal cross-checks (three shape measurement bands, 5 - 9 images of each source galaxy). If cross-checks among WFIRST-AFTA, Euclid, and LSST show that all of them are achieving statistics-limited WL measurements, then the combination of the three data sets will be considerably more powerful than any one in isolation. WFIRST-AFTA also provides deep near-IR imaging for photometric redshifts (in combination with LSST optical), and the galaxy redshift survey and special-purpose IFU observations may play an important role in photo- $z$  calibration.

While design studies and technology development are ongoing, the likely formal mission start for WFIRST is FY2017, provided that the NASA funding wedge opened by the completion of the *James Webb Space Telescope* returns to Astrophysics. The development schedule is 79 months, including 6 months of reserve, which would lead to launch in 2023. There is strong motivation in the astronomy community to maintain an early WFIRST launch so that there is overlap between its wide-field survey capability and JWST’s deep follow-up capability.

At the end of its 6-year prime mission, WFIRST-AFTA will remain an extraordinarily powerful facility for dark energy investigations, especially if internal tests demonstrate that the SN survey remains statistics-limited and that

single-band WL shape measurements are adequate. In this case, 2 – 4 years of observations in an extended mission could improve measurement precision on all axes by a factor of two, to confirm any surprising results from earlier studies and better characterize their physical implications. WFIRST-AFTA may thus remain an important part of the community’s dark energy portfolio through the 2020s and into the early 2030s.

More information about WFIRST can be found in

WFIRST-2.4: What Every Astronomer Should Know. Spergel, D., Gehrels, N., Breckinridge, J., Donahue, M., Dressler, A., Gaudi, B. S., et al. 2013, arXiv:1305.5425 [36]

Wide-Field InfraRed Survey Telescope-Astrophysics Focused Telescope Assets WFIRST-AFTA Final Report. Spergel, D., Gehrels, N., Breckinridge, J., Donahue, M., Dressler, A., Gaudi, B. S., et al. 2013, arXiv:1305.5422 [35]

Wide-Field InfraRed Survey Telescope (WFIRST) Final Report. Green, J., Schechter, P., Baltay, C., Bean, R., Bennett, D., Brown R., et al. 2012, arXiv:1208.4012 [34]

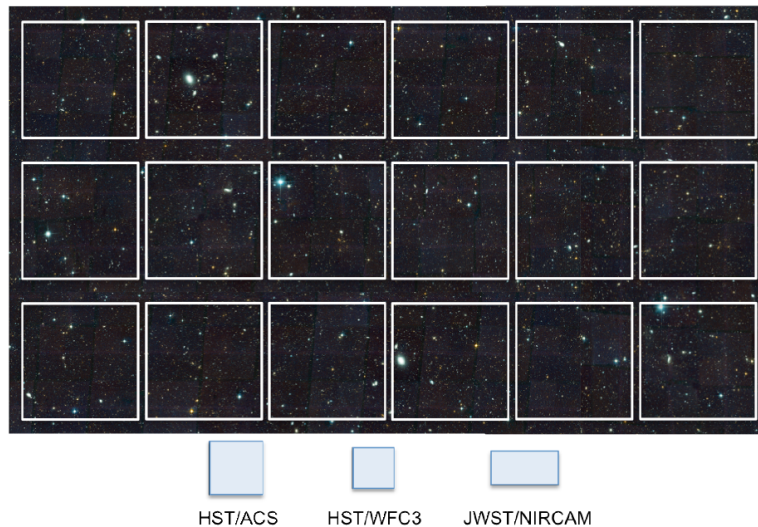


**Figure 6:** Field of view of the 300-Megapixel near-IR camera planned for WFIRST-AFTA. Each square is a  $4k \times 4k$  HgCdTe sensor array, with pixels mapped to 0.11 arcseconds on the sky. The field of view extent is  $0.79 \times 0.43$  degrees. This is  $\sim 200$  times the area of the IR channel on Hubble Space Telescope’s Wide Field Camera 3, which is shown to scale along with the fields of the largest imaging cameras on HST (optical) and the James Webb Space Telescope (IR).

## 11 Other Opportunities

The Facilities described in the preceding sections follow the “main line” of attack on dark energy outlined in the 2006 Dark Energy Task Force report, from Stage III experiments like BOSS and DES through to Stage IV experiments like DESI, LSST, Euclid, and WFIRST-AFTA. However, this list is by no means an exhaustive account of the experimental approaches being considered or, in some cases, actively pursued. We conclude this document with a brief overview of other kinds of facilities or experimental approaches that could play an important role in dark energy studies over the next 1-3 decades.

*Novel Probes of Gravity:* As discussed at length in the Snowmass white paper on this topic, there are many observational or laboratory approaches to testing modified gravity theories in addition to the expansion and growth measurements pursued by main-line dark energy experiments. These include precision tests of the equivalence principle, solar system GR tests, searches for time or spatial variation of fundamental “constants,” and tests of the effective strength of gravity in different astronomical environments.

*Local Calibration and Spectroscopic Follow-Up of Supernova Surveys:* The large-scale imaging facilities described above are powerful tools for discovery and photometric monitoring of supernovae. Fully exploiting these surveys requires accurate calibration against local supernova samples and spectroscopic follow-up of a significant fraction of the detected supernovae and/or their host galaxies. The follow-up campaigns have typically been *ad hoc* on a variety of telescopes, but the large size of upcoming imaging surveys may justify a more systematic approach. There has been great progress in constructing well characterized local calibrator samples in recent years, but continuing attention will be needed to maximize the payoff of future surveys.

*Deep Spectroscopic Surveys for Photometric Redshift Calibration:* Uncertainties in photometric redshift distributions are one of the most challenging systematics for weak lensing surveys. Cross-correlation of spectroscopic and imaging surveys (e.g., eBOSS/DES at Stage III and DESI/LSST at Stage IV) will be one important approach (see the Snowmass Cross-Correlation Report), but deep spectroscopic samples from large telescopes for optimizing algorithms and improving calibrations will also be crucial.

*Radio Surveys for BAO Measurements:* In addition to their optical and IR emission, galaxies can be detected by the 21cm radio emission from their neutral hydrogen gas. Because the BAO scale is large, radio interferometers can map large scale structure and measure BAO without resolving individual galaxies. This approach has significant technological challenges, particularly associated with controlling radio frequency interference and foregrounds, but it is potentially a very efficient way to map high-redshift BAO, and several experimental efforts are underway or planned.

*Balloon-Based Weak Lensing:* Euclid and WFIRST-AFTA will mark a major step in weak lensing by moving to the 0.1-arcsecond resolution that is achievable (over wide fields) only from space. A balloon-based experiment could make a first step into this high angular resolution regime by placing a wide field imaging platform above most of the atmospheric turbulence that affects ground-based images.

*Spectroscopic Follow-Up of LSST Imaging:* While the photometric redshifts from LSST imaging are sufficient for powerful weak lensing and BAO constraints, the precision on dark energy parameters would be amplified if moderate resolution spectroscopic redshifts were available for the bulk of the LSST sample. Novel instrumentation that might enable relatively inexpensive ground-based spectroscopy over wide fields, which could enable such an improvement, is now a subject of active investigation and development.

*Radio Weak Lensing:* A very ambitious radio facility like the envisioned Square Kilometer Array could make spatially resolved, 21cm velocity maps for hundreds of millions of galaxies. These kinematic measurements have the potential to reduce the shape noise in weak lensing measurements, and in the long run this approach might yield another leap forward in weak lensing precision beyond LSST, Euclid, and WFIRST-AFTA.

*Standard Sirens:* The gravity wave signals from merging black holes or neutron stars can be decoded to determine the distance to the source, providing a “standard siren” distance indicator that is rooted in fundamental physics rather than empirical correlations. A second-generation (post-LISA) space-based gravity wave interferometer could

achieve the sensitivity and angular resolution needed to detect merging compact binaries and unambiguously identify their galactic hosts over a large fraction of the observable universe. The limiting source of noise in these distance determinations would be gravitational lensing by intervening structure, which decreases at a predictable rate with increasing sample size. Samples of several hundred thousand sources are achievable in principle, which may yield the ultimate in precision measurement of cosmic acceleration.

## References

- [1] D. H. Weinberg, M. J. Mortonson, D. J. Eisenstein, C. Hirata, A. G. Riess, and E. Rozo, “Observational Probes of Cosmic Acceleration,” *Phys.Rept.* **530** (2013) 87–255, [arXiv:1201.2434 \[astro-ph.CO\]](#).
- [2] **SDSS Collaboration** Collaboration, K. N. Abazajian *et al.*, “The Seventh Data Release of the Sloan Digital Sky Survey,” *Astrophys.J.Suppl.* **182** (2009) 543–558, [arXiv:0812.0649 \[astro-ph\]](#).
- [3] J. A. Frieman, B. Bassett, A. Becker, C. Choi, D. Cinabro, *et al.*, “The Sloan Digital Sky Survey-II Supernova Survey: Technical Summary,” *Astron.J.* **135** (2008) 338–347, [arXiv:0708.2749 \[astro-ph\]](#).
- [4] H. Campbell, C. B. D’Andrea, R. C. Nichol, M. Sako, M. Smith, *et al.*, “Cosmology with Photometrically-Classified Type Ia Supernovae from the SDSS-II Supernova Survey,” *Astrophys.J.* **763** (2013) 88, [arXiv:1211.4480 \[astro-ph.CO\]](#).
- [5] **SDSS Collaboration** Collaboration, J. E. Gunn *et al.*, “The 2.5 m Telescope of the Sloan Digital Sky Survey,” *Astron.J.* **131** (2006) 2332–2359, [arXiv:astro-ph/0602326 \[astro-ph\]](#).
- [6] M. Sullivan, J. Guy, A. Conley, N. Regnault, P. Astier, *et al.*, “SNLS3: Constraints on Dark Energy Combining the Supernova Legacy Survey Three Year Data with Other Probes,” *Astrophys.J.* **737** (2011) 102, [arXiv:1104.1444 \[astro-ph.CO\]](#).
- [7] C. Heymans, L. Van Waerbeke, L. Miller, T. Erben, H. Hildebrandt, *et al.*, “CFHTLenS: The Canada-France-Hawaii Telescope Lensing Survey,” [arXiv:1210.0032 \[astro-ph.CO\]](#).
- [8] **SDSS Collaboration** Collaboration, D. J. Eisenstein *et al.*, “Spectroscopic target selection for the Sloan Digital Sky Survey: The Luminous red galaxy sample,” *Astron.J.* **122** (2001) 2267, [arXiv:astro-ph/0108153 \[astro-ph\]](#).
- [9] **SDSS Collaboration** Collaboration, D. G. York *et al.*, “The Sloan Digital Sky Survey: Technical Summary,” *Astron.J.* **120** (2000) 1579–1587, [arXiv:astro-ph/0006396 \[astro-ph\]](#).
- [10] **SDSS Collaboration** Collaboration, D. J. Eisenstein *et al.*, “Detection of the baryon acoustic peak in the large-scale correlation function of SDSS luminous red galaxies,” *Astrophys.J.* **633** (2005) 560–574, [arXiv:astro-ph/0501171 \[astro-ph\]](#).
- [11] **2dFGRS Collaboration** Collaboration, S. Cole *et al.*, “The 2dF Galaxy Redshift Survey: Power-spectrum analysis of the final dataset and cosmological implications,” *Mon.Not.Roy.Astron.Soc.* **362** (2005) 505–534, [arXiv:astro-ph/0501174 \[astro-ph\]](#).
- [12] S. Smee, J. E. Gunn, A. Uomoto, N. Roe, D. Schlegel, *et al.*, “The Multi-Object, Fiber-Fed Spectrographs for SDSS and the Baryon Oscillation Spectroscopic Survey,” [arXiv:1208.2233 \[astro-ph.IM\]](#).
- [13] **SDSS Collaboration** Collaboration, D. J. Eisenstein *et al.*, “SDSS-III: Massive Spectroscopic Surveys of the Distant Universe, the Milky Way Galaxy, and Extra-Solar Planetary Systems,” *Astron.J.* **142** (2011) 72, [arXiv:1101.1529 \[astro-ph.IM\]](#).
- [14] **BOSS Collaboration** Collaboration, K. S. Dawson *et al.*, “The Baryon Oscillation Spectroscopic Survey of SDSS-III,” [arXiv:1208.0022 \[astro-ph.CO\]](#).
- [15] L. Anderson, E. Aubourg, S. Bailey, D. Bizyaev, M. Blanton, *et al.*, “The clustering of galaxies in the SDSS-III Baryon Oscillation Spectroscopic Survey: Baryon Acoustic Oscillations in the Data Release 9 Spectroscopic Galaxy Sample,” *Mon.Not.Roy.Astron.Soc.* **427** no. 4, (2013) 3435–3467, [arXiv:1203.6594 \[astro-ph.CO\]](#).
- [16] A. G. Sanchez, C. Scoccola, A. Ross, W. Percival, M. Manera, *et al.*, “The clustering of galaxies in the SDSS-III Baryon Oscillation Spectroscopic Survey: cosmological implications of the large-scale two-point correlation function,” [arXiv:1203.6616 \[astro-ph.CO\]](#).
- [17] B. A. Reid, L. Samushia, M. White, W. J. Percival, M. Manera, *et al.*, “The clustering of galaxies in the SDSS-III Baryon Oscillation Spectroscopic Survey: measurements of the growth of structure and expansion rate at  $z=0.57$  from anisotropic clustering,” [arXiv:1203.6641 \[astro-ph.CO\]](#).
- [18] C. Alcock and B. Paczynski, “An evolution free test for non-zero cosmological constant,” *Nature* **281** (1979) 358–359.

- [19] N. G. Busca, T. Delubac, J. Rich, S. Bailey, A. Font-Ribera, *et al.*, “Baryon Acoustic Oscillations in the Ly- $\alpha$  forest of BOSS quasars,” *Astron.Astrophys.* **552** (2013) A96, [arXiv:1211.2616](#) [[astro-ph.CO](#)].
- [20] A. Slosar, V. Irsic, D. Kirkby, S. Bailey, N. G. Busca, *et al.*, “Measurement of Baryon Acoustic Oscillations in the Lyman-alpha Forest Fluctuations in BOSS Data Release 9,” *JCAP* **1304** (2013) 026, [arXiv:1301.3459](#) [[astro-ph.CO](#)].
- [21] **SDSS Collaboration** Collaboration, E. S. Sheldon *et al.*, “Cross-correlation Weak Lensing of SDSS Galaxy Clusters I: Measurements,” *Astrophys.J.* **703** (2009) 2217–2231, [arXiv:0709.1153](#) [[astro-ph](#)].
- [22] J. Bernstein, R. Kessler, S. Kuhlmann, R. Biswas, E. Kovacs, *et al.*, “Supernova Simulations and Strategies For the Dark Energy Survey,” *Astrophys.J.* **753** (2012) 152, [arXiv:1111.1969](#) [[astro-ph.CO](#)].
- [23] C. Blake and S. Bridle, “Cosmology with photometric redshift surveys,” *Mon.Not.Roy.Astron.Soc.* **363** (2005) 1329–1348, [arXiv:astro-ph/0411713](#) [[astro-ph](#)].
- [24] H.-J. Seo and D. J. Eisenstein, “Improved forecasts for the baryon acoustic oscillations and cosmological distance scale,” *Astrophys.J.* **665** (2007) 14–24, [arXiv:astro-ph/0701079](#) [[astro-ph](#)].
- [25] P. McDonald and U. Seljak, “How to measure redshift-space distortions without sample variance,” *JCAP* **0910** (2009) 007, [arXiv:0810.0323](#) [[astro-ph](#)].
- [26] P. McDonald and D. Eisenstein, “Dark energy and curvature from a future baryonic acoustic oscillation survey using the Lyman-alpha forest,” *Phys.Rev.* **D76** (2007) 063009, [arXiv:astro-ph/0607122](#) [[astro-ph](#)].
- [27] A. Albrecht and G. Bernstein, “Evaluating dark energy probes using multidimensional dark energy parameters,” *Phys.Rev.* **D75** (2007) 103003, [arXiv:astro-ph/0608269](#) [[astro-ph](#)].
- [28] M. Oguri and M. Takada, “Combining cluster observables and stacked weak lensing to probe dark energy: Self-calibration of systematic uncertainties,” *Phys.Rev.* **D83** (2011) 023008, [arXiv:1010.0744](#) [[astro-ph.CO](#)].
- [29] Z. Ivezić, T. Axelrod, W. Brandt, D. Burke, C. Claver, *et al.*, “Large Synoptic Survey Telescope: From Science Drivers To Reference Design,” *Serb.Astron.J.* **176** (2008) 1–13.
- [30] **LSST Science Collaborations, LSST Project** Collaboration, P. A. Abell *et al.*, “LSST Science Book, Version 2.0,” [arXiv:0912.0201](#) [[astro-ph.IM](#)].
- [31] **LSST Dark Energy Science Collaboration** Collaboration, A. Abate *et al.*, “Large Synoptic Survey Telescope: Dark Energy Science Collaboration,” [arXiv:1211.0310](#) [[astro-ph.CO](#)].
- [32] **EUCLID Collaboration** Collaboration, R. Laureijs *et al.*, “Euclid Definition Study Report,” [arXiv:1110.3193](#) [[astro-ph.CO](#)].
- [33] E. Majerotto, L. Guzzo, L. Samushia, W. J. Percival, Y. Wang, *et al.*, “Probing deviations from General Relativity with the Euclid spectroscopic survey,” *Mon.Not.Roy.Astron.Soc.* **424** (2012) 1392–1408, [arXiv:1205.6215](#) [[astro-ph.CO](#)].
- [34] J. Green, P. Schechter, C. Baltay, R. Bean, D. Bennett, *et al.*, “Wide-Field InfraRed Survey Telescope (WFIRST) Final Report,” [arXiv:1208.4012](#) [[astro-ph.IM](#)].
- [35] D. Spergel, N. Gehrels, J. Breckinridge, M. Donahue, A. Dressler, *et al.*, “WFIRST-2.4: What Every Astronomer Should Know,” [arXiv:1305.5425](#) [[astro-ph.IM](#)].
- [36] D. Spergel, N. Gehrels, J. Breckinridge, M. Donahue, A. Dressler, *et al.*, “Wide-Field InfraRed Survey Telescope-Astrophysics Focused Telescope Assets WFIRST-AFTA Final Report,” [arXiv:1305.5422](#) [[astro-ph.IM](#)].